Nanoparticle-Driven Intermolecular Cooperativity and Miscibility in Polystyrene/Poly(vinyl methyl ether) Blends

Avanish Bharati,[†,‡] Priti Xavier,[‡,§] Goutam Prasanna Kar,[§] Giridhar Madras,[†] and Suryasarathi Bose*[,§]

[†]Department of Chemical Engineering and [§]Department of Materials Engineering, Indian Institute of Science, Bangalore 560012, India

S Supporting Information

ABSTRACT: The effect of silver nanoparticles (nAg) in PS/PVME [polystyrene/poly(vinyl methyl ether)] blends was studied with respect to the evolution of morphology, demixing temperature, and segmental dynamics. In the early stage of demixing, PVME developed an interconnected network that coarsened in the late stage. The nAg induced miscibility in the blends as supported by shear rheological measurements. The physicochemical processes that drive phase separation in blends also led to migration of nAg to the PVME phase as supported by AFM. The segmental dynamics was greatly influenced by the presence of nAg due to the specific interaction of nAg with PVME. Slower dynamics and an increase in intermolecular cooperativity in the presence of nAg further supported the role of nAg in delaying the phase separation processes and augmenting the demixing temperature in the blends. Different theoretical models were assessed to gain insight into the dynamic heterogeneity in PS/PVME blends at different length scales.
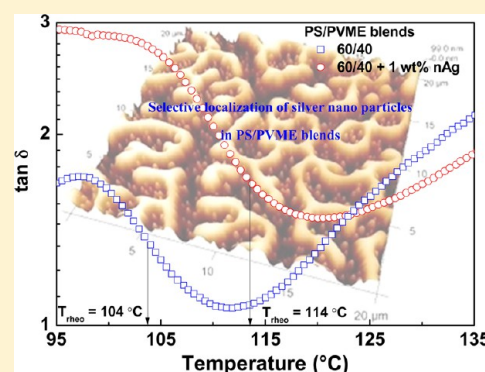
INTRODUCTION

In the domain of partially miscible polymer blends, dynamic asymmetry between the constituents leads to distinct phenomena such as localized cooperative molecular motion of the entities and a distribution of relaxation processes.[1] Often, a single glass transition temperature (T_g), as observed by differential scanning calorimetry (DSC), is interpreted as miscibility, although, down to molecular length scales, the local segmental dynamics is very different.

Various techniques (optical and electron microscopies, fluorescence and dielectric spectroscopies, dynamic light scattering measurements) have been employed in the recent past to evaluate the cloud-point temperature or turbidity in partially miscible polymeric systems. Although scattering experiments provide direct evidence of the cloud-point temperature, they are limited to samples that are optically transparent. In this regard, rheology has been quite useful. Although the region in the vicinity of demixing has been investigated, the mechanism of demixing is not yet fully understood. This might be due to the thermorheological complexity arising from the simultaneous interplay of kinetics, thermodynamics, and viscoelasticity.[2]

Polystyrene (PS)/poly(vinyl methyl ether) (PVME) blends are dynamically asymmetric in nature and often result in viscoelastic phase separation (VPS)[3] in which the minor phase initially forms a percolated network if it is more viscoelastic in nature.[4] The interaction parameter, χ, of PS/PVME is weakly negative.[5] A miscible polymer blend with such a large difference in T_g without strong specific interactions is thermorheologically complex[6] and exhibits both VPS and liquid–liquid phase separation (LPS). It was reported that, for 3.5–10 wt % PS in

PVME, viscoelasticity dominates thermodynamics in controlling the morphology and phase separation behavior.[7] In the early stage of spinodal decomposition, the concentration fluctuations lead to an increase in the storage modulus (G').[8] In the late stage of demixing, enhanced chain mobility dominates the overall viscoelastic properties.[9] Fredrickson and Larson[10] derived the contribution of concentration fluctuations to the evolving viscoelastic properties. However, the theory fails to correctly predict the temperature at which upturn occurs for off-critical compositions,[11] where the concentration fluctuations are weak.[12] New interfaces formed upon phase separation increase the elasticity, which explains the increase in the modulus for off-critical compositions.[13]

The advent of functional nanoparticles led to a paradigm shift in the field of polymer-based composites. It was realized that nanoparticles also stabilize the morphology of binary blends.[14] Lipatov et al.[15] reported that the addition of nanoparticles to a polymeric blend changes the interaction parameter between the components, because of which the components redistribute and, therefore, the phase separation temperature increases. Recently, Ginzburg[16] proposed a theory that elucidates the effects of spherical nanoparticles, on the order of the radius of gyration of polymer chains, on the demixing behavior in polymer blends. Hence, it could be quite interesting to systematically evaluate the effect of nanoparticles, on the order of the radius of gyration of macromolecules, on the demixing of polymer mixtures. More-

over, if the nanoparticles preferentially interact with one of the components, intriguing effects (such as the scale of cooperativity at T_g where chain connectivity is dominating and in the vicinity of demixing where thermal concentration fluctuation is dominating) are expected. By coupling dielectric spectroscopy and melt rheology, chain-connectivity effects at T_g and thermal concentration fluctuations can be deduced.[17]

Some results in our earlier work,[17] motivated us to systematically study the effect of silver nanoparticles (nAg) on the demixing behavior of PS/PVME blends especially when the particles (on the order of the radius of gyration of the entities) preferentially wet one of the phases. In this study, thermally induced phase separation in a dynamically asymmetric blend of PS/PVME with nAg was probed systematically using melt rheology, light microscopy, and dielectric spectroscopy in the temperature region near T_g and in the vicinity of demixing. By studying the segmental dynamics near T_g, the cooperativity of the chains can be assessed, which is crucial for understanding the thermodynamic concentration fluctuations especially in concentrated blends. For this purpose, 50/50 (w/w) and 60/40 (w/w) PS/PVME blends were chosen as the model systems in which concentration fluctuations are dominant. The evolution of viscoelastic properties was studied to evaluate the onset and late stage of phase separation. To evaluate the effect of nAg on the segmental dynamics and intermolecular cooperativity, dielectric spectroscopy was performed in situ as a function of temperature (near the glass transition of the blends) and frequency. The annealed and quenched morphologies and the localization of nAg were assessed using atomic force microscopy (AFM).

■ EXPERIMENTAL METHODS

Materials and Sample Preparation. PS with a weight-average molecular weight (M_w) of 35 kDa was obtained from Sigma-Aldrich, and PVME was supplied by TCI. The PVME had M_w and number-average molecular weight (M_n) values of 80 and 36.4 kDa, respectively, and was purified by a method described in our earlier work.[17] The silver nanoparticles (nAg) were supplied by Sigma-Aldrich and were used without any further surface treatment. The nAg particles were coated with PVP [poly-(vinylpyrrolidone)] to achieve a homogeneous dispersion in polar solvents. Analytical-grade solvents were obtained commercially and were used without further purification.

PS/PVME control blends in ratios of 50/50 (w/w) and 60/40 (w/w) without and with nAg (0.5 and 1 wt %) were prepared by solution mixing as described in our earlier work.[17] The weight of PVME was monitored prior to blend preparation, as PVME forms a lower critical solution temperature (LCST) system with water.[18,19]

Characterization. The nAg particles have a layer of PVP as a dispersant although the content is less than 0.5% (according to the supplier). Moreover, during the preparation of the blends in toluene, we expect PVP to dissolve in the solution. To verify this, we subjected the nAg (in toluene solution) to the same protocol as employed for preparing the blends, namely, probe sonication for 30 min followed by shear mixing for 45 min. Subsequently, the nAg sample was vacuum-dried, and XPS analyses were performed using an Axis Ultra (Kratos) spectrometer under a pressure that was typically around $(3-8) \times 10^{-9}$ Torr. The XPS data were collected using monochromatic Al Kα radiation at 1.486 keV operated at 150 W. The XPS spectrum (see Figure 1) shows two strong peaks of Ag $3d_{3/2}$ and Ag $3d_{5/2}$, and more importantly, the peak for N (of PVP) is absent, suggesting no/negligible PVP layer on the nAg after processing. This is
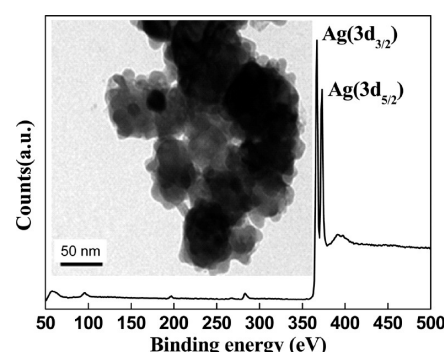

Figure 1. XPS spectrum of silver nanoparticles after processing (30 min of probe sonication and 45 min of shear mixing). Inset: TEM image of silver nanoparticles.

important for understanding the interactions between nAg and the constituents. We believe, according to XPS, that PVP might not influence the interactions between nAg and PVME (the most polar component in the blends).

Transmission electron microscopy (TEM; JEM-200CX) at 200 kV was used to study the dispersion state of nAg. Samples for TEM were prepared by ultrasonicating nAg in toluene for 30 min and depositing a drop on a holey carbon-coated copper grid. The inset of Figure 1 shows a TEM image of nAg. The average diameter was approximately 20−30 nm.

The glass transition temperatures were obtained from the step change in specific heat (C_p) recorded by a Mettler Toledo DSC instrument at a heating rate of 2 K/min. The samples were first heated to 80 °C and held at this temperature for 30 min before being quenched to −60 °C. The step change in C_p was recorded in the second heating run at 2 K/min.

The evolution of the viscoelastic properties as a function of temperature was monitored using a rheometer from TA Instruments (Discovery Hybrid-3). The detailed experimental procedure is described in our previous work.[17]

The phase-separated morphology was investigated by polarized optical microscopy (POM). The samples were heated at 1 K/min from the homogeneous state to the phase-separated regime. For neat blends, objective lenses of 20× magnification were used, whereas for blends with nAg, objective lenses of higher magnification (50×) were employed.

Impedance measurements were performed using an Alpha-N analyzer. For the measurements, films were deposited directly onto the electrodes. Solutions of 20 wt % were dissolved in toluene, drop cast onto the electrodes, allowed to dry at room temperature for two days, and then vacuum dried for two days. Phase-separated morphology was evaluated by AFM (Dimension Icon ScanAsyst) using soft tapping mode.

■ RESULTS AND DISCUSSION

Phase-Separated Morphology Assessed by POM and AFM. For POM, the thickness of the film was greater than the (i) radius of gyration (R_g) of the entities[20] and (ii) the maximum wavelength of concentration fluctuation (λ_m).[21] This was intended to minimize other parameters such as film thickness affecting the temperature of demixing. Figure 2 shows the morphology development in 50/50 (w/w) PS/PVME blends without (Figure 2a$_1$−a$_3$) and with (Figure 2b$_1$−b$_3$,c$_1$−c$_3$) nAg in the metastable and unstable regions due to modulation contrast. Because of the relative differences in the refractive indices of PS ($n_D = 1.592$) and PVME ($n_D = 1.467$) with respect to air ($n_D = 1$),
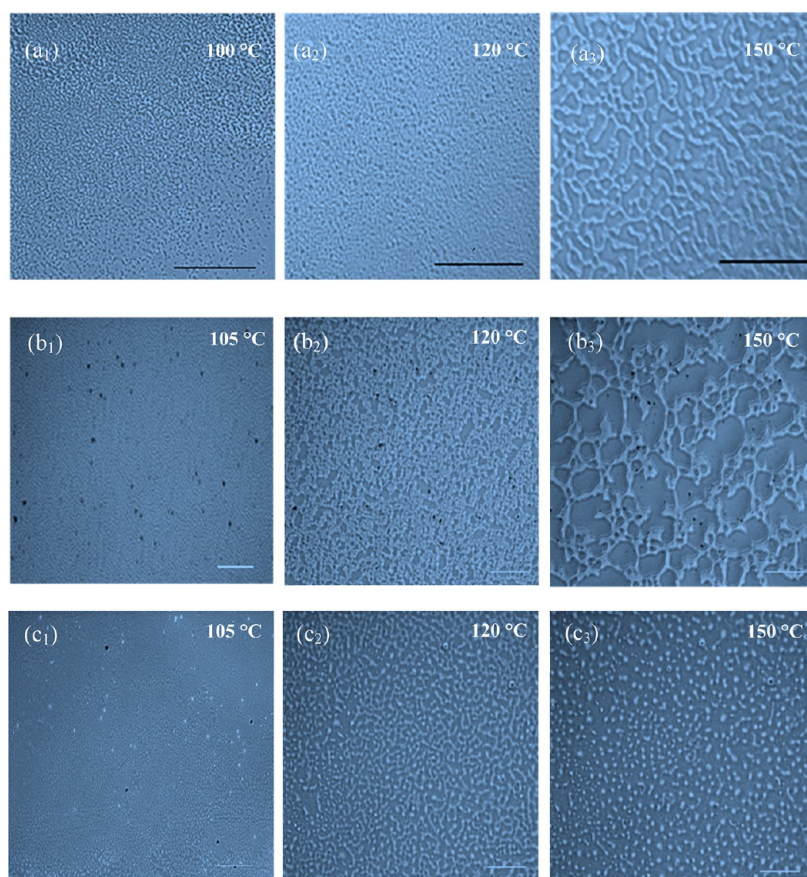
Figure 2. POM images of 50/50 PS/PVME blends with and without nAg during the (a_1, b_1, c_1) early, (a_2, b_2, c_2) intermediate, and (a_3, b_3, c_3) late stages of phase separation. The top row is for neat 50/50 PS/PVME blends. The middle and the bottom rows are for 50/50 PS/PVME blends with 0.5 and 1 wt % nAg, respectively. (The darker phase represents PS, and the brighter phase corresponds to the PVME phase. Black and white scale bars correspond to 100 and 20 μm, respectively.)

the bottom part (matrix) of the film appears dark, whereas the top portion appears bright.[22] Hence, PS appears darker, whereas PVME appears brighter. In the case of nAg, objective lenses with greater resolution were used. In the control 50/50 PS/PVME blends, a continuous structure of PVME developed in the metastable regions (Figure $2a_1$–a_3). This phenomenon is a typical characteristic of spinodal decomposition, where a sudden jump in concentration fluctuations results in an interconnected structure. The interconnected structure, though coarsened, was retained even in the unstable regions of the phase diagram (Figure $2a_3$). Interestingly, for the blends with nAg, a significant refinement in microstructure can be observed from Figure $2b_1$–b_3, c_1–c_3. This phenomenon is more prominent in 0.5 wt % nAg, where fine continuous threads of PVME are evident even in the late stage of demixing (Figure $2b_3$). However, at the higher concentration of nAg (1 wt %), the interconnected structure formed in the early stage coarsened into PVME-rich droplets (Figure $2c_3$), possibly as a result of selective localization of nAg in PVME (see discussion related to AFM).

In control 60/40 (w/w) PS/PVME blends, two intriguing observations demand attention. First, the PVME-rich phase coarsened into larger droplets, whereas the PS-rich phase formed the matrix in the early (Figure $3a_1$) and intermediate (Figure $3a_2$) stages of phase separation. Second, at a later stage, the PS phase transformed into disconnected domains in the PVME matrix. The enhancement in concentration fluctuations, especially in dynamically asymmetric blends, makes the slower component (PS) more viscoelastic than the faster component (PVME). In

the late stage of demixing, interfacial tension has little role to play, and the domain shape is contingent on the mechanical stress balance.[3,4] Selective localization of particles in a given phase of the blends can also alter the rheological properties and can manipulate the overall microstructure. In the case of 60/40 PS/PVME blends with 0.5 wt % nAg, the continuity of the PS phase was retained even in the late stage (Figure $3b_2, b_3$). In contrast, for 60/40 PS/PVME blends with 1 wt % nAg, the continuity of the more viscoelastic component coarsened in the late stage of phase separation. In VPS, it is believed that the volume shrinking of the PS-rich phase drives the coarsening process.[3,4] This phenomenon is also responsible for the decrease in the intensity of structure factor[4] and is manifested in retarding the correlation length (discussed in detail in the next section). As the blends studied here were of a near-critical nature, concentration fluctuations dominated the domain growth. The subsequent coalescence of PVME into larger domains (in the case of 60/40 PS/PVME blends) and the formation of a PS-rich matrix phase during the late stage of phase separation can very well be inferred for blends with nAg.

PVME selectively wets both the interfaces because of its lower interfacial tension[23] (29 mN/m) in comparison to that of PS (36 mN/m).[24] For blends that phase separate symmetrically, the phase separation occurs laterally and is accompanied by surface height variations as the faster component (PVME) migrates to the interface. Hence, PVME appears darker than PS, which forms the matrix in the AFM images. It is envisaged that in these blends, PVME preferentially enriches both the air and the substrate
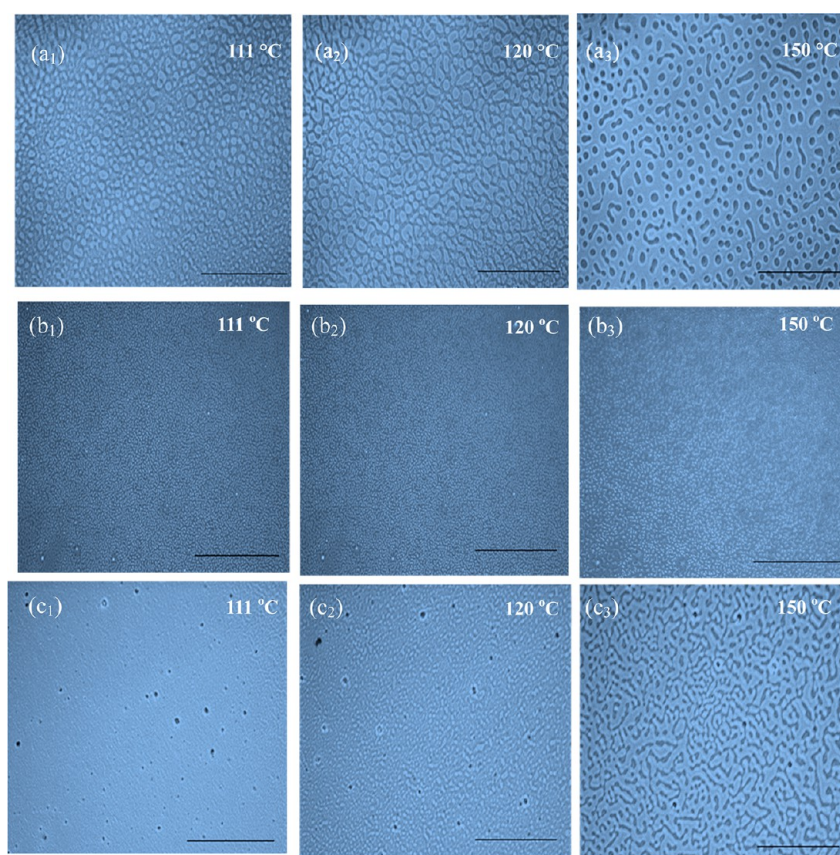
Figure 3. POM images of 60/40 PS/PVME blends with and without nAg during the (a_1,b_1,c_1) early, (a_2,b_2,c_2) intermediate, and (a_3,b_3,c_3) late stages of phase separation. The top row is for neat 60/40 PS/PVME blends. The middle and bottom rows are for 60/40 PS/PVME blends with 0.5 and 1 wt % nAg, respectively. (The darker phase represents PS, and the brighter phase corresponds to the PVME phase. Scale bar corresponds to 100 μm.)

interface. To verify this, XPS was performed on the annealed and phase-separated surfaces, as discussed later in this article.

Figure 4 presents phase and height images of phase-separated 50/50 and 60/40 PS/PVME blends with 1 wt % nAg. Annealed samples of 50/50 (w/w) blends with 1 wt % nAg for 2 h at 125 °C resulted in a cocontinuous morphology as seen from the AFM micrographs (Figure 4a). The domain size is comparable to that obtained from POM near the spinodal temperature (120 °C) for this particular composite. This can be explained by the slowing of the growth of domains by "pinning", when the characteristic domain size becomes comparable to the interparticle distance.[25] As stated, PVME is more polar than PS,[26] and PVME chains are preferentially absorbed on the surface of nanoparticles to minimize the free energy. In fact, phase images in Figure 4a,c show that nAg preferentially wets the PVME phase. Moreover, both the PS domains and the nAg appear brighter in the AFM micrographs. It is envisaged that, as the surface tension of nAg (~38 mN/m) is closer to that of PS, the phase contrasts of PS and nAg are similar, and their heights are almost the same as seen from the three-dimensional height images (Figure 4b−d). It is important to note that PVME preferentially wets both of the interfaces because of its lower interfacial tension, and hence, a thin layer of PVME-enriched surface is coated on the PS domains.[27] To verify this, we recorded XPS scans on phase-separated films, and interestingly, we detected PVME (see Figure 5) typically from the top 10 nm from the surface. A schematic representation showing the PVME enrichment in the phase-separated morphologies and the positioning of nAg in the blends is included in Figure 5 for better understanding.

Effect of nAg Particles on Long-Range Segmental Motion and Miscibility. To study the effect of nAg on long-range segmental motion, the glass transition temperature (T_g) was determined using a step change in C_p in DSC for 60/40 (w/w) blends without and with nAg (1 wt %) (see Figure 6). The initial, middle, and final points in the step change in C_p are indicated in the figure and listed in Table 1. The presence of a single T_g confirms that the system is homogeneous and also suggest that atactic PS with a random molecular configuration is miscible with PVME. The T_g value (considering the midpoint as T_g in the step change) decreased in the presence of nAg. The T_g value for the neat blends is consistent with the results reported by Schneider.[28] A large difference in the T_g values of the components investigated here also suggests a remarkable dynamic heterogeneity in the relaxation behavior and the dynamic segmental motions of the chains and is discussed in detail later in this article.

The macroscopic T_g value obtained closely fits the Brekner equation[29]

$$T_{gAeff}(\Phi_1) = T_{g2} + (T_{g1} - T_{g2})[(1 + K_1)\Phi_{1eff} \\ - (K_1 + K_2)\Phi_{1eff}^2 + K_2\Phi_{1eff}^3] \quad (1a)$$

where T_{g1eff} is the effective T_g value of polymer 1 and T_{g1} and T_{g2} are the glass transition temperatures of pure polymers 1 and 2, respectively. The values used for the parameter K_1 and K_2 were −0.707 and 0.462, respectively.[30] Φ_{eff} is the effective local concentration and was obtained using the expression
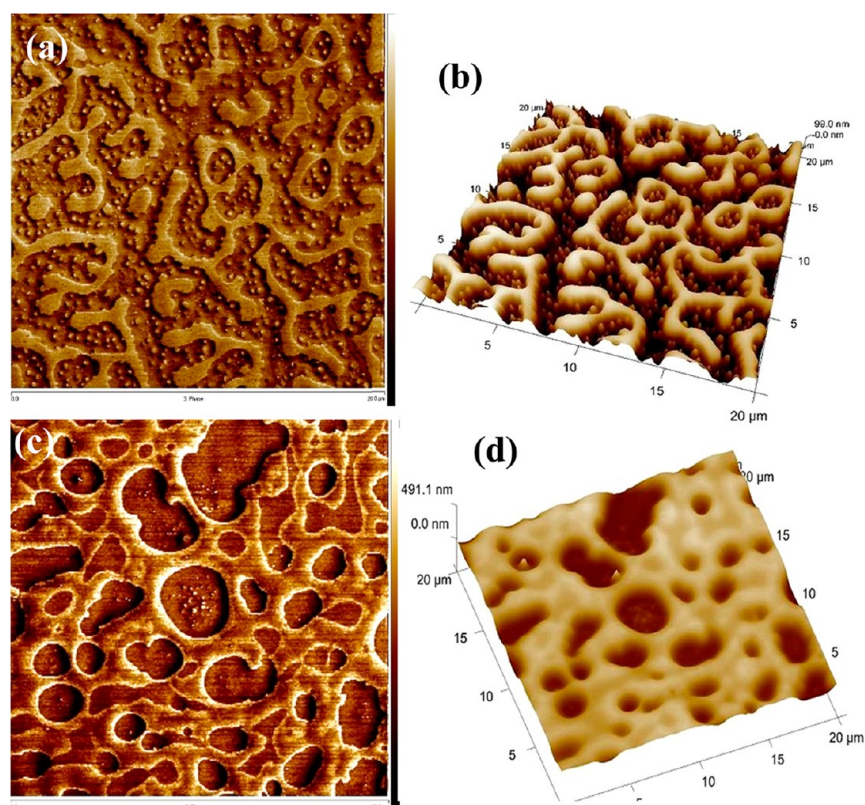
Figure 4. (a,c) Phase images and (b,d) three-dimensional height images of phase-separated blends: (a,b) 50/50 PS/PVME with 1 wt % nAg and (c,d) 60/40 PS/PVME with 1 wt % nAg. The darker phase is PVME, the brighter phase is PS, and the bright dots in the darker phase indicate the localization of nAg in PVME.

$$\Phi_{1\text{eff}} = \Phi_s + (1 - \Phi_s)\Phi_1 \tag{1b}$$

where Φ_s is self-concentration.[7] For macromolecules, fragility is a measure of intermolecular cooperativity and conformational changes in the glass transition region. The presence of nAg can significantly alter the conformational entropy of the chains. In addition, selective interaction with PVME can alter the overall segmental dynamics, as discussed in detail in subsequent sections.

Rheology in the Transition Regime: Effect of nAg Particles on the Concentration Fluctuation. The behaviors of the storage modulus (G') and tan δ for PS/PVME (60/40, w/w) blends with and without 1 wt % nAg are displayed in Figure 7. In the one-phase regime, G' decreases with increasing temperature. An increase in temperature moves the system away from the T_g value of the blends. This augments the polymer chain mobility (due to Brownian motion), which results in a decrease of G'. Dynamic asymmetry in PS/PVME, in turn, enhances the concentration fluctuations near the phase boundary.[31] The enhanced concentration fluctuations lead to the formation of dynamic domains that are rich in hard PS component and to a distinct change in the behavior of G' (as indicated in Figure 7a). As the stresses are of elastic origin, G' is more sensitive to demixing.[2,3]

The behavior of tan δ shows rather a different trend. The temperature at the maximum of dG'/dT or the minimum of $d(\tan \delta)/dT$ (as indicated in Figure 7b) is assigned as the rheologically determined demixing temperature (T_{rheo}). Interestingly, with the addition of nAg (1 wt %), T_{rheo} shifts to a higher temperature by ca. 10 °C (Figure 7b), essentially suggesting that nAg favors the mixing of the polymers. This observation is found

to be consistent with increasing the concentration of nAg for both compositions and is listed in Table 2. The higher concentration of nAg (2 wt %) resulted in a decrease in the phase separation temperature (not shown here), where particle aggregation possibly dominated the overall phase separation behavior. It is envisaged that the particle-rich phase might phase separate differently than the bulk, as a random network of particle segregation governs the viscoelastic behavior of the system instead of concentration fluctuations.[32]

PVME (polar solubility parameter, $\delta_p = 7.1$ MPa$^{1/2}$) is more polar than PS ($\delta_p = 1.1$ MPa$^{1/2}$).[26] Hence, PVME has more affinity toward nAg, as also supported by AFM observations. The mobility of the adsorbed polymer segments decreases near the nAg surface when the size of the nanoparticles is on the order of the radius of gyration of the polymer (R_g) (12.3 nm for PS and 11.5 nm for PVME).[20] The regions of adsorbed layers retard the overall dynamics of the polymer segments and increase G' in filled systems, especially at low frequencies.[33]

Recently, Ginzburg[16] proposed a thermodynamic model to illustrate the effect of hard spherical nanoparticles on the spinodal temperature of polymer blends comprising two homopolymers. The theory suggests[16] that the free energy per unit volume comprises the free energy from the mixing of the binary blend, entropic contributions from nanoparticle interactions, and enthalpic and entropic contributions from polymer−nanoparticle interactions.

In our study, R_p (radius of the particle) of nAg (∼20−30 nm as seen from TEM) is comparable with the R_g of PS and PVME (12.3 nm for PS and 11.5 nm for PVME[20]). This reduces the number of unfavorable PS−PVME interactions, increases the critical value of the degree of segregation, and thus decreases the
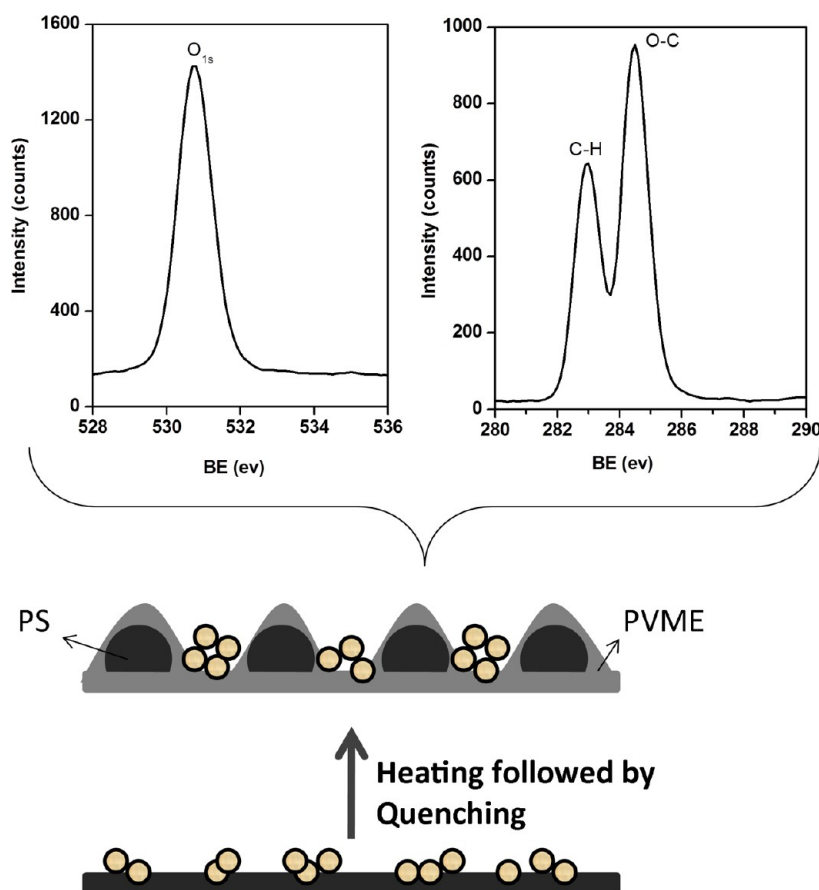
Figure 5. Schematic representation of the PVME-enriched surface layer in phase-separated PS/PVME blends. Inset: XPS scans from the surface.
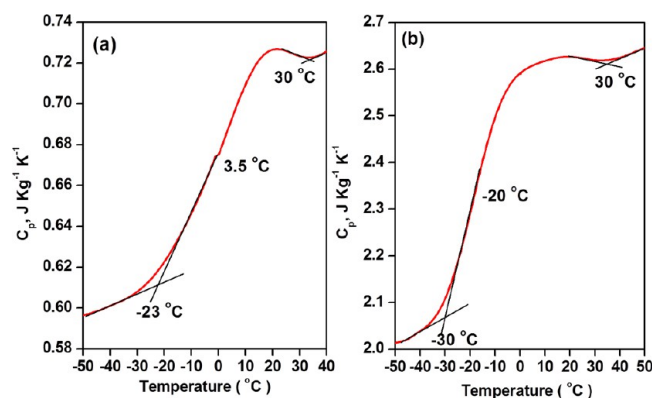

Figure 6. DSC thermograms of 60/40 blends: (a) without and (b) with 1 wt % nAg.

enthalpic fraction of the free energy. In addition, smaller nanoparticles have higher translational entropy than the polymer. These factors are responsible for increasing the miscibility of PS/PVME blends in the presence of nAg.

Spinodal temperature can be determined by the method Ajji and Choplin[34] based on dynamic temperature ramp measurements. This method is an extension of the theoretical approach of Larson and Fredrickson[35] and is extensively used for calculating the dynamic moduli due to concentration fluctuations of polymer blends near phase separation. The expressions for G' and G'' are

$$G' = \frac{k_B T \omega^2}{1920} \left\{ \frac{1}{3} \left[\frac{R_{g1}^2}{\Phi N_1} + \frac{R_{g2}^2}{(1-\Phi)N_2} \right] \right\}^{1/2}$$

$$\left[\frac{1}{\Phi a_1^2 W_1} + \frac{1}{(1-\Phi)a_2^2 W_2} \right]^2 [2(\chi - \chi_s)]^{-5/2} \quad (2a)$$

$$G'' = \frac{k_B T \omega}{240} \left\{ \frac{1}{3} \left[\frac{R_{g1}^2}{\Phi N_1} + \frac{R_{g2}^2}{(1-\Phi)N_2} \right] \right\}^{-1/2}$$

$$\left[\frac{1}{\Phi a_1^2 W_1} + \frac{1}{(1-\Phi)a_2^2 W_2} \right]^2 [2(\chi - \chi_s)]^{-5/2} \quad (2b)$$

Table 1. Glass Transition Temperature (T_g) Obtained Using DSC and Volume and Scale of Cooperativity for Different Compositions

sample	T_{gi} (°C)	T_{gmid} (°C)	T_{gf} (°C)	ΔC_p^{-1} [(J K^{-1} g^{-1})$^{-1}$]	volume of cooperativity[a] V_a (Å^3)	scale of cooperativity[b] r_a (Å)
PS/PVME 60/40	−23	3.5	30	6.4	92	4.5
PS/PVME 60/40 + 1 wt % nAg	−30	−20	30	5.7	396	7.3

[a]Calculated using eq 12c. [b]$r_a = (V_a)^{1/3}$.

2219

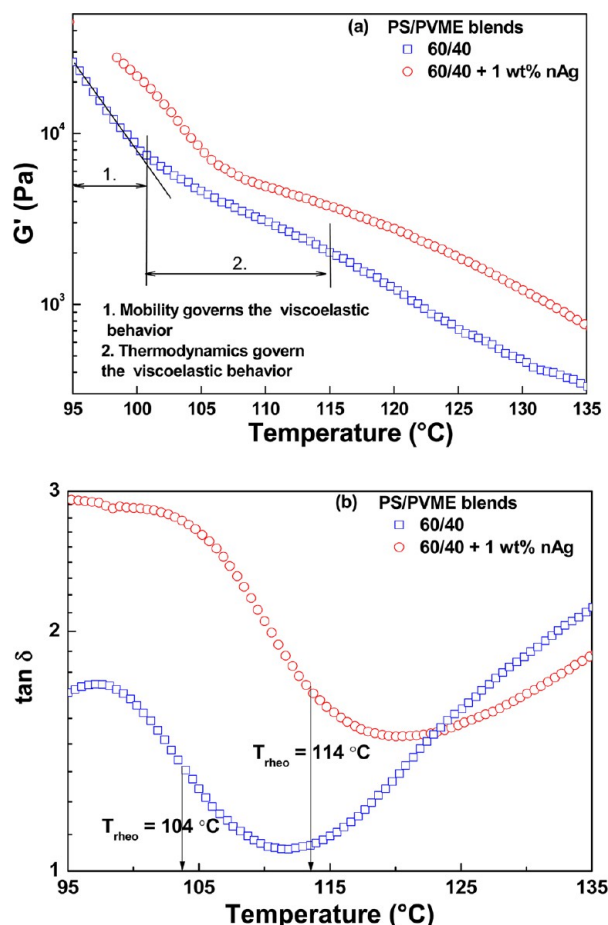dx.doi.org/10.1021/jp4112712 | J. Phys. Chem. B 2014, 118, 2214−2225

Figure 7. Isochronal (ω = 0.1 rad/s) dynamic temperature ramp performed at 1% strain with a 0.5 °C/min heating rate: (a) G' vs temperature and (b) tan δ vs temperature plots for 60/40 PS/PVME blends with and without nAg (1 wt %).

Table 2. Comparison of Binodal, Spinodal, and Rheological Demixing Temperatures Obtained by Various Rheological Techniques and Interaction Parameters[a] for Different Compositions

composition	T_{rheo} (±2 °C)	$T_s{}^b$ (±2 °C)	$T_s{}^c$ (±2 °C)	$T_b{}^d$ (±2 °C)	calculated interaction parameter χ (×10³)
50/50	104	110	111	103	–
50/50 + 0.5 wt % nAg	106	119	119	104	–
50/50 + 1 wt % nAg	108	120	120	105	–
60/40	104	112	111	102	4.51
60/40 + 0.5 wt % nAg	114	121	120	107	3.45
60/40 + 1 wt % nAg	114	121	120	108	3.44

[a]Obtained from equality of the chemical potentials of components in the two phases. [b]Obtained from eq 4 [from the intercept of the reciprocal square of the correlation length (ξ^{-2}) versus temperature]. [c]Obtained from the intercept of $(G''^2/TG')^{2/3}$ versus 1/T. [d]Obtained from Figure 8.

where Φ is the volume fraction; R_{gi} is the radius of gyration of species i, defined as $R_{gi}{}^2 = N_i a_i{}^2/6$; χ and χ_s denote the interaction parameter and the interaction parameter at the spinodal point. N_i

is the number of segments of type i. W_i denotes the rate of motion of the subunit of length a_i. By plotting $(G''^2/TG')^{2/3}$ versus $(1/T)$, the spinodal temperature (T_s) can thus be obtained from the intercept (not shown here). Table 2 lists the T_s values obtained using this method for the blends investigated here. Fredrickson and Larson's theory considers only the anomalous contribution to the shear stress caused by critical fluctuations in homogeneous polymer melts. One has to take into account the background moduli, where no thermodynamic effects interfere and assume that the measured moduli and the background moduli have the same temperature dependence to estimate the spinodal temperature. However, it is envisaged that shear rheological measurements are adequate in providing information on the phase diagram. Although this is still debatable, we made an attempt to estimate T_s from the reciprocal of the correlation length (ξ), a quantity that can be derived directly from isochronal temperature scans.

The correlation length can be obtained using the equation

$$\xi = \left(\frac{k_B T}{30\pi} \frac{G'}{G''^2}\right)^{1/3} \qquad (3)$$

As an example, Figure 8 elucidates the behavior of the correlation length (ξ) near the phase separation region. The data plotted
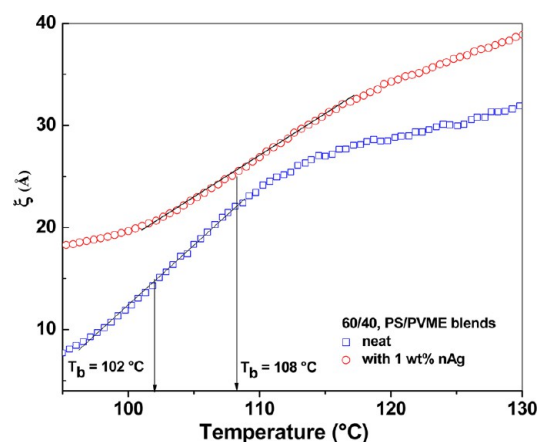

Figure 8. Plot of correlation lengths for 60/40 PS/PVME blends with and without nAg (1 wt %).

here were determined using the temperature ramp data of Figure 7. In the vicinity of phase separation, ξ changes rapidly as a function of temperature. Often, the binodal temperature is taken where a distinct change in ξ is noticed (also indicated in Figure 8). At the onset of demixing, ξ progressively increases as a result of local concentration fluctuations, whose magnitude increases in the presence of nAg. This might be due to favorable polymer–filler interactions, which, in this case, represent PVME–nAg interactions. The temperature at which the ξ increases rapidly is delayed in the case of nAg, suggesting that the filler induces miscibility in the system. The sudden rise in the correlation length for 50/50 (w/w) and 60/40 (w/w) blends suggests that the demixing in the blends is faster. The rate of increase in the correlation length in the case of blends with nAg is lower than that in the neat polymer blend, suggesting that particles slow the phase separation process. The stated hypothesis is also validated by the POM images (Figures 2 and 3). The ξ value obtained in this work is in close agreement with the results of Dudowicz and Freed[36] and Han et al.[5] A comparison of binodal temperatures obtained using temperature ramp measurements (Figure 7) and

from the variation of ξ with temperature (Figure 8) is summarized in Table 2.

In the vicinity of phase separation $\xi(T,\varphi)$ might have a scaling form as often observed in critical fluctuation phenomenon

$$\xi(T, \varphi) = \xi_o(\varphi)\varepsilon^{-n} \tag{4}$$

where $\varepsilon = [(T - T_c)/T_c]$ and $n = \frac{1}{2}$ as per the mean-field model.

In Figure 9, the reciprocal of the square of the correlation length (ξ^{-2}) is plotted as a function of temperature for various
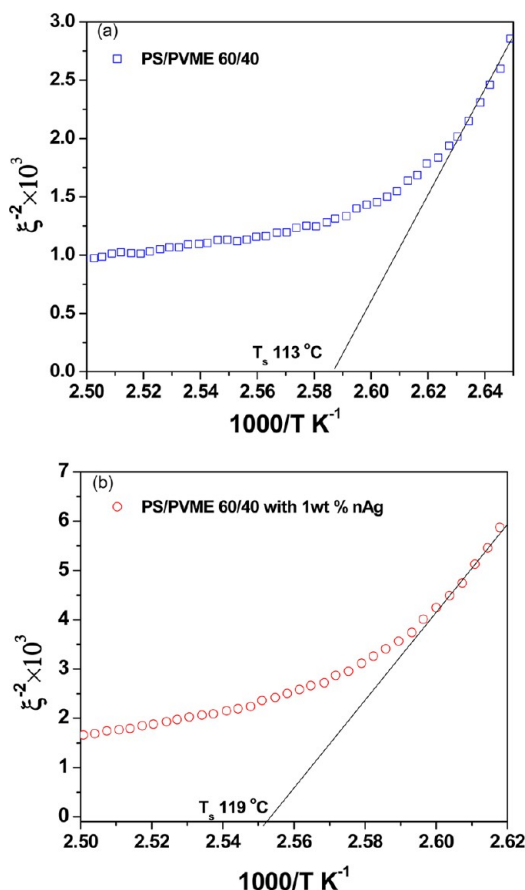

Figure 9. Reciprocal correlation length as a function of frequency for 60/40 PS/PVME blends: (a) control and (b) with 1 wt % nAg.

blends. A straight line interpreting $\xi^{-2} = 0$ can be taken as the spinodal decomposition temperature (T_s).

We have made an attempt to deduce the variance in the concentration fluctuation from isochronal temperature sweeps using melt rheology with the equation

$$\langle\delta\Phi^2\rangle = S(0)/\xi^2 R_c \tag{5}$$

The low entropy of mixing, which is inversely related to chain length, causes the concentration fluctuations in weakly interacting blends to prevail several hundreds of degrees from the critical point. However, the present consensus is that the local concentration fluctuations are affected by both concentration fluctuations (intrachain, self-concentration; interchain, thermal concentration) and chain connectivity effects. Recently, Shenogin et al.[30] proposed a model that suggests that the local composition variations determine the distributions of segmental dynamics. They modeled the Gaussian distribution function of the effective concentration surrounding a polymer segment in terms of intrachain and interchain contributions. Interestingly,

the size of the correlation volume for the sampling of concentration fluctuations is composition-independent and is sufficient to quantitatively predict experimental data with only weak temperature dependence. Because $\xi > R_c$, the model reasonably predicted the data for PS/PVME with a considerably smaller volume, whose diameter is comparable to the Kuhn length (l_K), in agreement with Lodge and McLeish.[37] For small correlation volumes $(\check{R} < 0.3)$, where $\check{R} = R_c/\xi$, which are prevalent in weakly interacting blends, the simplified mean squared concentration fluctuations is given by

$$\langle\delta\Phi^2\rangle = \frac{3\sqrt{v_A v_B}}{2\pi R_c}\left(\frac{b_A^2}{\varphi_A} + \frac{b_B^2}{\varphi_B}\right)^{-1} \tag{6a}$$

$$\xi^2 = \frac{S(0)}{12}\left(\frac{b_A^2}{\varphi_A} + \frac{b_B^2}{\varphi_B}\right) \tag{6b}$$

Using eqs 6a and 6b, the variation of mean squared concentration fluctuation with temperature is plotted in Figure S1 (see the Supporting Information), which explains the decreasing trend of the mean squared concentration fluctuation with temperature. Interestingly, a significant departure from the linear slope of the mean squared concentration fluctuation was observed at binodal temperatures (T_b) for the PS/PVME (60/40) blend both without and with 1 wt % nAg. A rapid decrease in the slope persisted in the metastable region that saturated after the spinodal temperature (T_s), which essentially suggests that the concentration fluctuations are weak above T_s. Moreover, as can be seen from Figure S1 (Supporting Information), the concentration fluctuations persist several degrees above T_g.

We now attempt to evaluate the Flory−Huggins interaction parameter taking into account the bound polymer adsorbed onto the surface of nAg. First, we obtain the phase diagram from isochronal dynamic temperature sweeps for various compositions. It is believed that the flow does not interfere with the demixing processes in isochronal sweeps as the strains used are low enough to lie in the terminal regime.[13,38]

Selective adsorption of PVME chains on the surface of nAg decreases the PVME fraction in PS/PVME blend in comparison to unfilled blends. The amount of bound polymer can be calculated using the following relationship proposed by Cohen-Addad[39]

$$w_{BdR} = \frac{\sqrt{\overline{M_0}}}{A_0}\frac{cS}{\varepsilon_a}\frac{\sqrt{\overline{M_n}}}{N_{av}} \tag{7a}$$

where $\overline{M_0}$ is the weight of bound nAg per gram mole of the polymer, A_0 is the average area associated with one noncovalent bond with PVME (equal to 0.1 nm^2 for N molecule corresponding to a 150-pm van der Waal radius), $\varepsilon_a \approx 1$, c is the filler concentration, M_n is the number-average molecular weight of the polymer, S is the specific surface area of filler, and N_{av} is Avogadro's number (6.023 × 10^{23} mol^{-1}). The weight fraction of PVME after the incorporation of nAg satisfies the relation

$$w_{PVME} = (1 - w_{BdR})w_{PVME}^0 \tag{7b}$$

where w_{PVME} and w_{PVME}^0 are the weight fractions of PVME in the bulk after and before the introduction of nAg, respectively. For small spherical particles, the excess absorbed polymer chains per unit surface area change the bound volume fraction of polymer on nAg, which leads to a decrease in the interaction parameter

(see Figure S2, Supporting Information) and to miscibility. This is in accordance with the values obtained for the interaction parameter calculated on equating the chemical potentials of components 1 and 2 in the two phases, summarized as

$$\chi_1 = \frac{\ln\left(\frac{\phi_1'}{\phi_1''}\right) + \left(1 - \frac{r_1}{r_2}\right)(\phi_2' - \phi_2'')}{r_1(\phi_2''^2 - \phi_2'^2)} \quad (8a)$$

$$\chi_2 = \frac{\ln\left(\frac{\phi_2'}{\phi_2''}\right) + \left(1 - \frac{r_2}{r_1}\right)(\phi_1' - \phi_1'')}{r_1(\phi_1''^2 - \phi_1'^2)} \quad (8b)$$

where

$$\chi = (\chi_1 + \chi_2)/2 \quad (8c)$$

The interaction parameters were obtained from DSC by employing the Gordon–Taylor (G–T) equation.[29] The phase composition of component 1 in phase a is obtained using the rearrangement of the G–T equation

$$W_{1a} = \frac{-k(T_{gB}^a - T_{g2})}{(T_{gB}^a - T_{g1}) - k(T_{gB}^a - T_{g2})} \quad (8d)$$

where $k = \Delta\alpha_2/\Delta\alpha_1$ and $\Delta\alpha = \rho\Delta C_p$. Using the phase compositions, ΔC_p, and obtained T_g, χ values were calculated using the above equations and are summarized in Table 2. The values obtained are in close agreement with the χ values obtained using the bound volume approach (see Figure S2, Supporting Information).

As discussed, in a polymer blend (of concentration φ) where the two components are chemically bound to two segments, the effective local concentrations φ_{effA} and φ_{effB} are given by[40]

$$\varphi_{effA} = \varphi_{sA} + (1 - \varphi_{sA})\varphi \quad (8e)$$

$$\varphi_{effB} = \varphi_{sB} + (1 - \varphi_{sB})(1 - \varphi) \quad (8f)$$

where φ_{sA} and φ_{sB} are the respective self-concentrations.

In the domain of polymer blends, the size of the relevant volume of the segmental dynamics is very small, on the order of l_K^3, where l_K is the Kuhn length, and hence, φ_s is close to 1, and therefore, $\varphi_{eff} \approx 1$. The model proposed by Lodge and McLeish[41] considered l_K as the relevant length scale for segmental dynamics. However, if this scale is significantly larger, chain connectivity effects are negligible. On the other hand, if the spatial heterogeneity is on the order of time scale of the segmental dynamics, thermal concentration fluctuations can elucidate the relaxation broadening of the component (here, PVME). It is envisaged that, at temperatures near the T_g value of the blends, the dynamics of some PVME segments are faster than that of the pure polymer, in an environment of frozen PS.[42] In the presence of nAg, the segmental relaxation of PVME is slowed. It is noteworthy that, at higher temperature, the concentration fluctuations are weak, the response of each component can be probed, and the distinct segmental mobility is apparent.

For PS/PVME system, the radius (R_c) of the cooperative volume V in the temperature range of $T_g + 20\,K < T < T_g + 60\,K$ is in the range of few nanometers, which increases in size when approaching the glass transition temperature.[43] However, in general, the surface concentration (here adsorbed PVME on nAg) decreases with decreasing particle radius (nAg diameters are on the order of 20–30 nm) because of smaller numbers of contacts at the curved surface, leading to a smaller adsorption

energy (χ_s).[44] This phenomenon, in fact, results in a larger volume that is available per adsorption site and is associated with small demixing entropy. For strong polymer–particle interactions (in this case, between nAg and PVME), the amount of excess adsorbed polymer chains per unit surface area is larger for smaller particles,[44] which further increases the critical value of the degree of segregation, χN, and thus decreases the enthalpic fraction of the free energy. The effective volume V_{eff} (in blends with particles) is large. Because of this selective adsorption of PVME onto nAg, the cooperative relaxation volume V increases, as the blend T_g value increases. Further analysis is required in this regard to experimentally deduce the effect of particles, on the order of radius of gyration of the chains, on V_{eff} and the segmental dynamics and is the subject of future investigations.

Dielectric Spectroscopy: Segmental Relaxations, Coupling, and Intermolecular Cooperativity. Dielectric spectroscopy measurements were performed to study the effect of nAg on the segmental relaxations and intermolecular cooperativity in the blends. PVME reorients more rapidly to an alternating ac field than PS.[22] By probing the dynamics around T_g, intermolecular cooperativity can be assessed.

Figure 10 depicts the frequency dependence of ε'' in the temperature range where the segmental dynamics is active in the
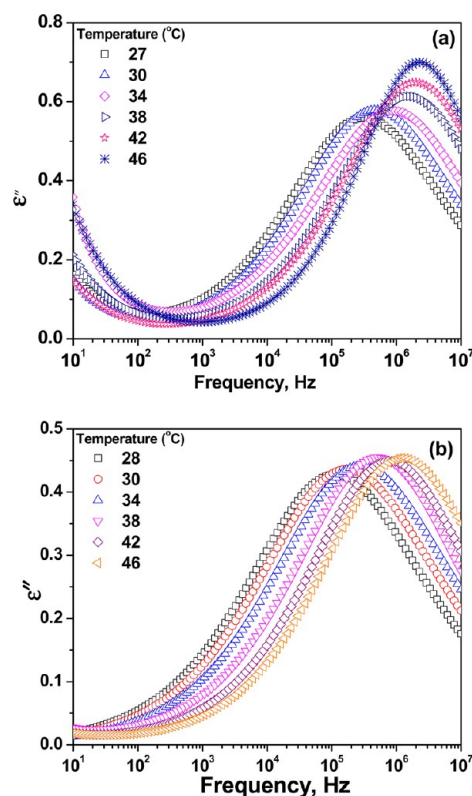

Figure 10. Dielectric loss (ε'') as a function of frequency for 60/40 PS/PVME blends: (a) without and (b) with 1 wt % nAg.

frequency window for control PS/PVME blends (60/40, w/w) and blends with nAg (1 wt %). The HN fitting parameters of the isothermal modulus scans (depicted in Figure 10) are compiled in Table S1 (Supporting Information). The broadness of the relaxation is explained by the parameter α, and the skewness is characterized by parameter β. Above T_g, a main loss peak at higher frequencies that depends strongly on temperature and corresponds to the segmental dynamics (α-relaxation) is very

evident. Debye-type relaxations are obvious in neat blends, with the values of both parameters close to unity.[20,45] In the case of blends with nAg, the segmental relaxations are observed to be significantly altered (see Figure 10b). For instance, the main loss maxima of the blends are shifted toward lower frequencies, suggesting a slowing of the PVME dynamics. PVME is more polar than PS, and hence, nAg is preferentially localized in the PVME phase of the blends. Near the calorimetric T_g, the chain segments of the slower component could be considered immobile with respect to the time scale of motion of the component with the lower T_g value. The origin of anomalous broadening of the glass transition in dielectric spectra of miscible polymer blends is the distribution of segment environments. This is attributed to the T_g dependence on composition stimulated by concentration fluctuations,[37] which is a measure of the degree to which the neighboring chain segments affect the relaxation of a polymer segment. However, we can appreciate this change marginally here due to the limited temperature range measured.

Different theoretical models have been proposed to explain the heterogeneous nature of the α-relaxation process. Fischer and co-workers[43] formulated their approach on the basis that disparities in T_g promote differences in relaxation rates of the polymer segments. The other approach considers that concentration fluctuations govern the segmental dynamics. Moreover, the difference between the coupling between the molecules and their surroundings is a direct measure of the relaxation shape, which forms the basis of framework of the coupling model (CM).[46] The intermolecular cooperativity in polymer blends can further be studied by comparing the coupling parameters, n, with that of the neat blend, given in eq 9.[47] The method of analysis used is based on the HN equation. The width of the relaxation function in the time domain is well-described by Kohlrausch–Williams–Watts (KWW) model. The following equations were reported to calculate the KWW parameters from the HN fittings

$$\beta_{KWW} = (\alpha\gamma)^{1/1.23}, \qquad n = 1 - \beta_{KWW} \tag{9}$$

A smaller β_{KWW} value suggests a broader distribution of relaxation time, whereas a higher β_{KWW} value implies a narrower distribution. It is evident from Table S1 (Supporting Information) that β_{KWW} decreased in the presence of nAg, indicating increased intermolecular cooperativity. This is further manifested from the coupling parameter n in Figure 11a.

The temperature dependence of the relaxation times for the investigated systems can be elucidated by the Vogel–Fulcher (VF) equation[48]

$$\tau = \tau_0 \exp\left(\frac{DT_o}{T - T_o}\right) \tag{10}$$

where T_o is the Vogel temperature and D is a material parameter associated with the apparent activation energy. As the frequency–temperature dependency in this work is quite linear, it can be described better by the Arrhenius equation, given by

$$\tau = A \exp\left(\frac{-E_a}{RT}\right) \tag{11}$$

where E_a (kJ/mol) is the activation energy.

The results indicate that E_a is lower in the case of blends with nAg (Figure 11b,c). A lower E_a value can also be related to an increased free volume. This is further manifested in a lower T_g in the case of blends with nAg. Often, hastened segmental dynamics
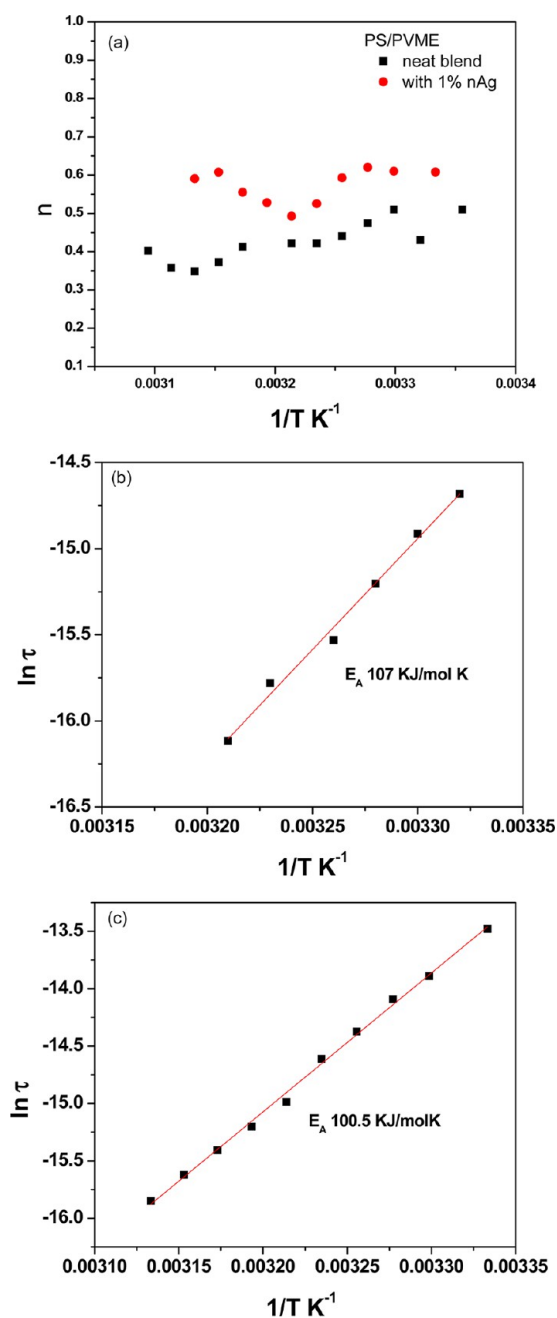

Figure 11. (a) Intermolecular coupling in 60/40 PS/PVME blends without and with 1 wt % nAg. (b,c) Activation energies for 60/40 PS/PVME blends: (b) without and (c) with 1 wt % nAg.

due to increased free volume is associated with a lower energy barrier. This also leads to lower intermolecular cooperativity; however, in our case, we observed a retardation of the dynamics and also moderately improved intermolecular cooperativity in the presence of nAg (see Figure 11a). It is important to recall that blends with nAg enhanced the miscibility in the blends, which is contingent on enhanced intermolecular interactions between the components. Hence, lower T_g and activation energy values in the case of blends with nAg hint at different environments: local confinement of chains in the vicinity of nAg in striking contrast to the bulk. The free volumes in the two environments are also different. Shear rheology represents macroscopic length scales in comparison to dielectric spectroscopy, which represents microscopic length scales. Using the coupling model, the dependency

of the apparent relaxation time on the strength of intermolecular constraints, n, and the local friction coefficient (from τ_0) can be explained. Interestingly, although the homopolymers PS and PVME have similar coupling constants, the large difference in the calorimetric T_g values of the components facilitates the study of the effect of interchain coupling on the shape and temperature dependence of the segmental relaxations.[49]

According to AG (Adam Gibbs) theory, cooperativity is believed to increase with decreasing temperature and is expressed as

$$\tau = \tau_o \exp\left[\frac{N_A s_c^* \Delta\mu}{k_B T S_c(T)}\right] \quad (12a)$$

where $\Delta\mu$ is the elementary activation energy, N_A is Avogadro's number, and $S_c(T)$ is the macroscopic configurational entropy. ΔC_p decreases with increasing temperature,[50] and hence, $S_c(T)$ can be expressed as

$$S_c(T) = \frac{N_A s_c^* \Delta\mu}{k_B T \ln[\tau(T)/\tau_o]} \quad (12b)$$

From the heat capacity increment at T_g, $\Delta C_p(T)$ can be extracted. Once $\Delta C_p(T_g)$ is evaluated, the values of $\Delta\mu$ can be derived. Hence, by assuming a value of s_c^* ($k_B \ln 3!$), a relation between $S_c(T)/\Delta\mu$ can be derived. It is interesting to note that macroscopic configurational entropy diminishes slowly with decreasing temperature (see Figure S3 of the Supporting Information). This also essentially means that the number of particles that cooperatively rearrange is assumed to increase with decreasing temperature. Interestingly, the $S_c(T)/\Delta\mu$ values in the case of blends with nAg are lower than those of control blends, indicating a loss in configurational entropy.

The scale of cooperativity at T_g can be expressed as

$$V_a = k T_g^2 \Delta C_p^{-1}/\rho(\delta T)^2 \quad (12c)$$

where ρ is the density of the bulk material, ΔC_p^{-1} is the relaxation strength of the reciprocal specific heat at constant pressure, and δT is the half-width of the glass transition temperature. Interestingly, the scale of cooperativity in the case of blends with 1 wt % nAg is higher than that of the neat blends. This is also manifested from the lower T_g values in the blends.[51]

In conclusion, from the dielectric spectroscopic analysis near T_g, it is clear that addition of nAg enhances the intermolecular cooperativity/coupling moderately. The decrease in the activation energy in the presence of nAg can be viewed as a consequence of the increased length over which cooperativity is required.

CONCLUSIONS

The effect of nAg on the viscoelastic phase separation and critical temperature of demixing of a dynamically asymmetric blend, PS/PVME, was studied using melt rheology and dielectric spectroscopy for near-critical compositions. Significant changes in long-range segmental motions were observed in the presence of nAg. Moreover, the spinodal demixing temperature was augmented by ca. 10 °C in the blends in the presence of nAg. The evolution of the morphology at different stages of phase separation was studied using POM, and the phase-separated morphologies were evaluated using AFM. In the early stage of phase separation, PVME formed an interconnected network, which was retained for longer time scales in the presence of nAg and was observed to be a function of the concentration of nAg.

Dielectric spectroscopy detected the presence of heterogeneity at temperatures even below the demixing temperature. The local segmental dynamics of the chain segments were significantly influenced in the presence of nAg. The latter effect was attributed to the selective interaction of nAg with PVME, which was also supported by AFM. An increase in relaxation time and activation energy further supported the key role of nAg in retarding the phase separation processes and augmenting the miscibility in the blends.

ASSOCIATED CONTENT

Ⓢ Supporting Information

Summary of HN fitting parameters (Table S1), variation in mean squared concentration fluctuation with temperature for 60/40 PS/PVME blends without and with 1 wt % nAg (Figure S1), interaction parameters for both the PS-rich and PVME-rich phases (Figure S2), and configurational entropy for blends with and without nAg (Figure S3). This material is available free of charge via the Internet at http://pubs.acs.org.

AUTHOR INFORMATION

Corresponding Author
*E-mail: sbose@materials.iisc.ernet.in. Tel.: +91-80-22933407.
Author Contributions
‡A.B. and P.X. contributed equally to this work.
Notes
The authors declare no competing financial interest.

ACKNOWLEDGMENTS

REFERENCES

(1) Takeno, H.; Kobayashi, M.; Aikawa, T. Localized Cooperative Molecular Motion in Miscible Polymer Mixtures with Large Difference in Glass-Transition Temperatures. *Macromolecules* **2006**, *39*, 2183−2190.

(2) Khademzadeh, Y. J.; Goharpey, F.; Foudazi, R. Can Only Rheology Be Used To Determine the Phase Separation Mechanism in Dynamically Asymmetric Polymer Blends (PS/PVME)? *RSC Adv.* **2012**, *2*, 8116−8127.

(3) Tanaka, H. Universality of Viscoelastic Phase Separation in Dynamically Asymmetric Fluid Mixtures. *Phys. Rev. Lett.* **1996**, *76*, 787−790.

(4) Tanaka, H. Unusual phase separation in a polymer solution caused by asymmetric molecular dynamics. *Phys. Rev. Lett.* **1993**, *71*, 3158−3161.

(5) Han, C. C.; Bauer, B. J.; Clark, J. C.; Muroga, Y.; Matsushita, Y.; Okada, M.; Tran-cong, Q.; Chang, T.; Sanchez, I. C. Temperature, Composition and Molecular-Weight Dependence of the Binary Interaction Parameter of Polystyrene/Poly(vinyl methyl ether) Blends. *Polymer* **1988**, *29*, 2002−2014.

(6) Zhang, H.; Lamnawar, K.; Maazouz, A. Rheological Modeling of the Mutual Diffusion and the Interphase Development for an Asymmetrical Bilayer Based on PMMA and PVDF Model Compatible Polymers. *Macromolecules* **2012**, *46*, 276−288.

(7) Khademzadeh, Y. J.; Goharpey, F.; Foudazi, R. Rheology and Morphology of Dynamically Asymmetric LCST Blends: Polystyrene/Poly(vinyl methyl ether). *Macromolecules* **2010**, *43*, 8670−8685.

(8) Zhang, R.; Cheng, H.; Zhang, C.; Sun, T.; Dong, X.; Han, C. C. Phase Separation Mechanism of Polybutadiene/Polyisoprene Blends under Oscillatory Shear Flow. *Macromolecules* **2008**, *41*, 6818−6829.

(9) Kapnistos, M.; Hinrichs, A.; Vlassopoulos, D.; Anastasiadis, S. H.; Stammer, A.; Wolf, B. A. Rheology of a Lower Critical Solution Temperature Binary Polymer Blend in the Homogeneous, Phase-Separated, and Transitional Regimes. *Macromolecules* **1996**, *29*, 7155−7163.

(10) Fredrickson, G. H.; Larson, R. G. Viscoelasticity of Homogeneous Polymer Melts near a Critical Point. *J. Chem. Phys.* **1987**, *86*, 1553−1560.

(11) Bousmina, M.; Lavoie, A.; Riedl, B. Phase Segregation in SAN/PMMA Blends Probed by Rheology, Microscopy, and Inverse Gas Chromatography Techniques. *Macromolecules* **2002**, *35*, 6274−6283.

(12) Kim, J. K.; Son, H. W. The Rheological Properties of Polystyrene/Poly(vinyl methyl ether) Blend near the Critical Region and in the Homogenous Region. *Polymer* **1999**, *40*, 6789−6801.

(13) Niu, Y. H.; Wang, Z. G. Rheologically Determined Phase Diagram and Dynamically Investigated Phase Separation Kinetics of Polyolefin Blends. *Macromolecules* **2006**, *39*, 4175−4183.

(14) Bose, S.; Özdilek, C.; Leys, J.; Seo, J. W.; Wübbenhorst, M.; Vermant, J.; Moldenaers, P. Phase Separation as a Tool to Control Dispersion of Multiwall Carbon Nanotubes in Polymeric Blends. *ACS Appl. Mater. Interfaces* **2010**, *2*, 800−807.

(15) Lipatov, Y. S.; Nesterov, A.; Ignatova, T.; Nesterov, D. Effect of Polymer−Filler Surface Interactions on the Phase Separation in Polymer Blends. *Polymer* **2002**, *43*, 875−880.

(16) Ginzburg, V. V. Influence of Nanoparticles on Miscibility of Polymer Blends. A Simple Theory. *Macromolecules* **2005**, *38*, 2362−2367.

(17) Xavier, P.; Bose, S. Multiwalled-Carbon-Nanotube-Induced Miscibility in Near-Critical PS/PVME Blends: Assessment through Concentration Fluctuations and Segmental Relaxation. *J. Phys. Chem. B* **2013**, *117*, 8633−8646.

(18) Suzuki, M.; Hirasa, O. An Approach to Artificial Muscle Using Polymer Gels Formed by Micro-Phase Separation. *Adv Polym. Sci.* **1993**, *110*, 241−261.

(19) El-Mabrouk, K.; Belaiche, M.; Bousmina, M. Phase Separation in PS/PVME Thin and Thick Films. *J. Colloid Interface Sci.* **2007**, *306*, 354−367.

(20) Pathak, J. A.; Colby, R. H.; Floudas, G.; Jerome, R. Dynamics in Miscible Blends of Polystyrene and Poly(vinyl methyl ether). *Macromolecules* **1999**, *32*, 2553−2561.

(21) Cahn, J. W. On Spinodal Decomposition. *Acta Metall.* **1961**, *9*, 795−801.

(22) Polios, I. S.; Soliman, M.; Lee, C.; Gido, S. P.; Schmidt-Rohr, K.; Winter, H. H. Late Stages of Phase Separation in a Binary Polymer Blend Studied by Rheology, Optical and Electron Microscopy, and Solid State NMR. *Macromolecules* **1997**, *30*, 4470−4480.

(23) Yurekli, K.; Karim, A.; Amis, E. J.; Krishnamoorti, R. Influence of Layered Silicates on the Phase-Separated Morphology of PS−PVME Blends. *Macromolecules* **2003**, *36*, 7256−7267.

(24) Pan, D. H. K.; Prest, W. Surfaces of Polymer Blends: X-ray Photoelectron Spectroscopy Studies of Polystyrene/Poly(vinyl methyl ether) Blends. *J. App. Phys.* **1985**, *58*, 2861−2870.

(25) Ginzburg, V. V.; Qiu, F.; Paniconi, M.; Peng, G.; Jasnow, D.; Balazs, A. C. Simulation of Hard Particles in a Phase-Separating Binary Mixture. *Phys. Rev. Lett.* **1999**, *82*, 4026−4029.

(26) Yurekli, K.; Karim, A.; Amis, E. J.; Krishnamoorti, R. Phase Behavior of PS−PVME Nanocomposites. *Macromolecules* **2004**, *37*, 507−515.

(27) Ermi, B. D.; Karim, A.; Douglas, J. F. Formation and Dissolution of Phase-Separated Structures in Ultrathin Blend Films. *J. Polym. Sci. B: Polym. Phys.* **1998**, *36*, 191−200.

(28) Schneider, H. A. Glass Transition Behaviour of Compatible Polymer Blends. *Polymer* **1989**, *30*, 771−779.

(29) Gordon, M.; Taylor, J. S. Ideal Copolymers and the Second Order Transitions of Synthetic Rubbers. I. Non-Crystalline Copolymers. *J. App. Chem.* **1952**, *2*, 493−500.

(30) Shenogin, S.; Kant, R.; Colby, R. H.; Kumar, S. K. Dynamics of Miscible Polymer Blends: Predicting the Dielectric Response. *Macromolecules* **2007**, *40*, 5767−5775.

(31) Sharma, J.; Clarke, N. Miscibility Determination of a Lower Critical Solution Temperature Polymer Blend by Rheology. *J. Phys. Chem. B* **2004**, *108*, 13220−13230.

(32) Gao, J.; Huang, C.; Wang, N.; Yu, W.; Zhou, C. Phase Separation of Poly(methyl methacrylate)/Poly(styrene-co-acrylonitrile) Blends in the Presence of Silica Nanoparticles. *Polymer* **2012**, *53*, 1772−1782.

(33) Pryamitsyn, V.; Ganesan, V. Origins of Linear Viscoelastic Behavior of Polymer−Nanoparticle Composites. *Macromolecules* **2006**, *39*, 844−856.

(34) Ajji, A.; Choplin, L. Rheology and Dynamics near Phase Separation in a Polymer Blend: Model and Scaling Analysis. *Macromolecules* **1991**, *24*, 5221−5223.

(35) Larson, R.; Fredrickson, G. H. Viscometric Properties of Block Polymers near a Critical Point. *Macromolecules* **1987**, *20*, 1897−1900.

(36) Dudowicz, J.; Freed, K. F. Correlation Lengths and Chain Sizes in PS/PVME Blends: Influence of Compressibility, Interactions, and Monomer Structures. *J. Chem. Phys.* **1992**, *96*, 1644−1647.

(37) Gibbs, J. H.; DiMarzio, E. A. Nature of the Glass Transition and the Glassy State. *J. Chem. Phys.* **1958**, *28*, 373−383.

(38) Takahashi, Y.; Suzuki, H.; Nakagawa, Y.; Noda, I. Effects of Shear Flow on Viscoelastic Properties of Polystyrene/Poly(vinyl methyl ether) Blends near the Phase Separation Temperature. *Macromolecules* **1994**, *27*, 6476−6481.

(39) Cohen-Addad, J. Silica−Siloxane Mixtures. Structure of the Adsorbed Layer: Chain Length Dependence. *Polymer* **1989**, *30*, 1820−1823.

(40) Leroy, E.; Alegría, A.; Colmenero, J. Segmental Dynamics in Miscible Polymer Blends: Modeling the Combined Effects of Chain Connectivity and Concentration Fluctuations. *Macromolecules* **2003**, *36*, 7280−7288.

(41) Lodge, T. P.; McLeish, T. C. Self-Concentrations and Effective Glass Transition Temperatures in Polymer Blends. *Macromolecules* **2000**, *33*, 5278−5284.

(42) Cendoya, I.; Alegría, A.; Alberdi, J. M.; Colmenero, J.; Grimm, H.; Richter, D.; Frick, B. Effect of Blending on the PVME Dynamics. A Dielectric, NMR, and QENS Investigation. *Macromolecules* **1999**, *32*, 4065−4078.

(43) Zetsche, A.; Fischer, E. Dielectric Studies of the α-Relaxation in Miscible Polymer Blends and Its Relation to Concentration Fluctuations. *Acta Polym.* **1994**, *45*, 168−175.

(44) Piculell, L.; Viebke, C.; Linse, P. Adsorption of a Flexible Polymer onto a Rigid Rod. A Model Study. *J. Phys. Chem.* **1995**, *99*, 17423−17430.

(45) Cheng, Y.-T.; Uang, R.-H.; Chiou, K.-C. Effect of PVP-coated Silver Nanoparticles Using Laser Direct Patterning Process by Photothermal Effect. *Microelectron. Eng.* **2011**, *88*, 929−934.

(46) Roland, C.; Ngai, K. Segmental Relaxation in Miscible Polymer Blends. *J. Rheol.* **1992**, *36*, 1691.

(47) Zhang, S.; Painter, P. C.; Runt, J. Coupling of Component Segmental Relaxations in a Polymer Blend Containing Intermolecular Hydrogen Bonds. *Macromolecules* **2002**, *35*, 9403−9413.

(48) Chehrazi, E.; Taheri Qazvini, N. Nanoconfined Segmental Dynamics in Miscible Polymer Blend Nanocomposites: The Influence of the Geometry of Nanoparticles. *Iran. Polym. J.* **2013**, *22*, 613−622.

(49) Roland, C.; Ngai, K. Segmental Relaxation and the Correlation of Time and Temperature Dependencies in Poly(vinyl methyl ether)/Polystyrene Mixtures. *Macromolecules* **1992**, *25*, 363−367.

(50) Roland, C.; Ngai, K. Segmental Relaxation and Molecular Structure in Polybutadienes and Polyisoprene. *Macromolecules* **1991**, *24*, 5315−5319.

(51) Katana, G.; Fischer, E.; Hack, T.; Abetz, V.; Kremer, F. Influence of Concentration Fluctuations on the Dielectric α-Relaxation in Homogeneous Polymer Mixtures. *Macromolecules* **1995**, *28*, 2714−2722.